Presented at 15th Workshop on Crystalline Silicon Solar Cells & Modules: Materials and Processes
Vail Colorado, USA, 7-10 August, 2005

PASSIVATING MULTI CRISTALLINE Si SOLAR CELLS USING SiN_x:H

I. G. Romijn, W. J. Soppe, H. C. Rieffe, W. C. Sinke, A. W. Weeber
ECN Solar Energy, P. O. Box 1, 1755 ZG Petten, The Netherlands
email: romijn@ecn.nl

ABSTRACT:

Passivating solar cells with SiN_x:H has been so far a scarcely understood effect that can only be optimized for cell production in an empirical way. In this study we determine the structural properties of SiN_x:H layers with Fourier Transform Infrared (FTIR) measurements and relate these to both the deposition parameters and its passivating qualities for solar cells. Furthermore we determined the relations between the hydrogen diffusion in the SiN_x:H and the structural properties of these layers.

The Si-N, Si-H and N-H bond densities for layers deposited with either nitrogen (N_2), ammonia (NH_3) or deuterated ammonia (ND_3|) and silane (SiH_4) are affected by the N/Si flow ratio and the pressure *p* in a similar way although the differences in dissociation energy and rate cause different deposition mechanisms. Comparing the Si-N and Si-H bond densities found for NH_3 and ND_3 grown layers, we find that roughly 25% of the hydrogen in the SiN_x:H layers stems from the ammonia precursor gas, while 75% stems from the silane.

We show that Si-N bond density is an important parameter governing both the bulk and surface passivation of the SiN_x:H layers. In spite of the different deposition mechanisms, the same relations hold between the H-diffusion coefficient, Si-N bond density and passivating qualities of SiN_x:H layers deposited with either N_2 or NH_3. The best bulk and surface passivating layers have a relatively low hydrogen diffusion coefficient due to a high Si-N bond density. We find optimum values for bulk and surface passivation for Si-N bond densities of $1.3*10^{23}$ cm^{-3}, regardless of the type of SiN_x:H used and regardless of the starting wafer quality. Lower Si-N bond densities result in layers with a more open structure and this will probably lead to H_2 formation during annealing. These H_2 molecules will effuse into the ambient during firing, and do not contribute to the passivation of solar cells. Higher Si-N bond densities result in a too dense structure, prohibiting an effective diffusion of H-atoms into the bulk of the solar cells. This study further indicates that FTIR analysis gives us a quick and reliable tool to check the quality and properties of SiN_x:H layers. This will allow optimization of SiN_x:H deposition systems without having to make complete solar cells.

1 INTRODUCTION

Hydrogenated amorphous silicon nitride layers (a-SiN_x:H) have become a very important part of modern silicon PV technology. They act as an anti-reflection coating and provide both bulk and surface passivation, important means for optimizing multi crystalline (mc) Si solar cells and obtaining high efficiencies [1]. The bulk, or defect passivation is achieved by driving hydrogen into the mc Si solar cells by a short thermal anneal [2,3,4]. At the same time, the surface passivation is improved by reducing the number of dangling bonds and creating a positive field effect by K+ centers [5].

On of the key issues of our research is to combine excellent bulk and surface passivation on low cost silicon with easy-to-handle gasses. Relations between structural properties and the quality of bulk and surface passivation of SiN_x:H need to be known for better understanding of the underlying physics. So far, passivation with SiN_x:H in industry has been a phenomenon that can only be optimized for cell production in an empirical way. This study provides means to determine passivating qualities of SiN_x:H independently of the deposition method and without making solar cells.

The amount of hydrogen diffusion from the SiN_x:H layer into the silicon wafer largely determines the quality of bulk passivation. Numerous generic studies of hydrogen diffusion in silicon nitride films have been reported [6,7,8,9], but studies on the relation between hydrogen diffusion in silicon nitride and bulk passivation are rather scarce [10,11]. The surface passivation is commonly related to the refractive index [5,12] and not to the structural properties. Only Mäckel and Lüdemann [13] and ECN [14] performed such a study. In recent publications, Weeber et al. [14,15] presented a systematic investigation on the bulk and surface passivating properties, the hydrogen loss mechanism in the SiN_x:H layer, and related these to the structural properties of the SiN_x:H deposited with SiH_4 and N_2. This first study is now extended to the use of NH_3 and deuterated ammonia (ND_3). The use of ND_3 sheds more light on the plasma chemistry and the deposition mechanisms of the SiN_x:H layer, while the use of both N_2 and NH_3 nitrides on solar cells reveals the structural properties of the SiN_x:H

layers that govern its inherent passivating qualities independent of the deposition mechanisms.

2 EXPERIMENTAL

2.1 Approach

The physics behind the passivating properties of SiN_x:H layers is investigated in four steps:

- Deposition of layers on double polished Cz Si wafers for FTIR analysis to obtain bond densities, and relating those to the deposition parameters;
- Application of the examined layers to solar cells; determination of bulk passivating quality by measuring V_{oc} and the Internal Quantum Efficiency at 1000 nm ($IQE_{(1000nm)}$), and relating these to the structural properties;
- Application of the examined layers to FZ Si wafers; determination of surface passivation by measuring the effective lifetime (τ_{eff}) using the Quasi Steady State Photo Conductance method [16] and relating these to the structural properties;
- Annealing of SiN_x layers for increasing time periods at 800 ºC to determine H-diffusivity in the SiN_x:H layer and relate that to the structural properties of SiN_x:H;

2.2 Deposition of SiN_x:H layers

We deposited SiN_x:H layers with three different types of nitrogen-containing precursor gases; nitrogen (N_2), ammonia (NH_3) and deuterated ammonia (ND_3). This will allow us to determine whether fundamental relations exist independent of the process gases. Silane (SiH_4) was used as silicon precursor gas. The SiN_x:H layers were deposited using the in-line microwave remote Plasma Enhanced Chemical Vapor Deposition (MW RPECVD) system at ECN at different process parameters such as pressure and gas flows. This MW RPECVD has been co-developed with Roth and Rau [17].

2.3 FTIR analysis

We determined the bond densities (Si-H, Si-H and N-H) within the nitride layers using FTIR spectroscopy. From the transmission spectrum of the SiN_x:H layers deposited on Si substrates the absorption spectrum (k) of the single layer of SiN_x:H was calculated according to the method reported by Maley [18]. Subsequently, the bond densities are calculated by integrating the different absorption peaks and multiplying them with a proper proportionality constant [19,20].

2.4 Solar cells

The mc Si solar cells for the determination of the bulk passivation were made using neighboring wafers; the process sequence was: texturing using acidic etching, emitter formation using an infrared heated belt furnace, remote MW PECVD of SiN_x:H using the same deposition parameters as for the FTIR samples, metallization using screen printing and contact formation with an infrared heated belt furnace. IV measurements were performed with our Class A solar simulator according to the ASTM-E948 norm; the Internal Quantum Efficiency (IQE) was calculated from the spectral response and the reflectance.

3. EXPERIMENTAL RESULTS AND DISCUSSION

3.1 SiN_x:H structural properties related to the deposition parameters

In previous studies it was found that the mass density of the SiN_x:H layers is related to the Si-N bond density: layers containing more Si-N bonds have a higher mass density ρ, while those with relatively more Si-Si bonds are less dense and have a more porous structure [14, 21, 22].

In figure 1 and 2 the Si-N bond density for three nitrides deposited with NH_3, ND_3 and N_2 as precursor gasses are shown as a function of the N/Si gas flow ratio, and for different deposition pressures. For all nitrides the Si-N bond densities increase for increasing N/Si flow ratio, and are higher for lower deposition pressures. The refraction index n increases with decreasing Si-N bond density and decreasing N/Si flow ratio, which is shown qualitatively by the arrow in the graphs.

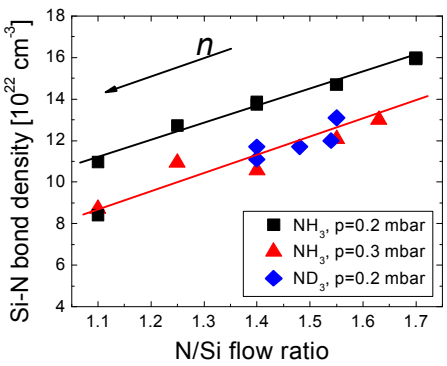

Figure 1: Si-N bond density versus the N/Si flow ratio for nitrides deposited with NH_3 and ND_3 at different pressures.

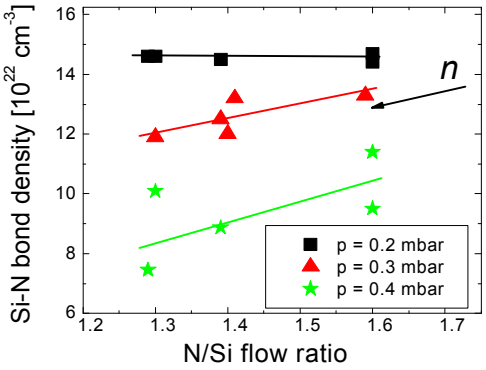

Figure 2: Si-N bond density vs N/Si flow ratio for nitrides deposited with N_2 at different pressures.

In figure 3 and 4 the Si-H and N-H bond densities of the same SiN_x:H layers are shown. For the Si-H and N-H bond densities of the NH_3 and ND_3 nitrides (figure 3) no pressure dependence is found; the Si-H bond density decreases, while the N-H bond density increases with increasing gas flow ratio. The Si-H and N-H bond densities of the N_2 nitrides however, do not significantly depend on the N/Si flow ratio. For these bond densities we see the pressure dependence as a main effect repeated. The points in figure 4 are averages over all values at a certain pressure.

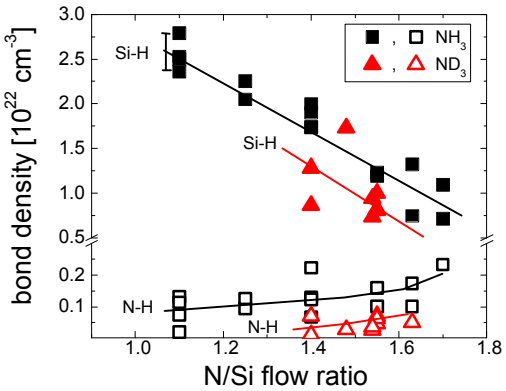

Figure 3: Si-H and N-H bond density versus the N/Si flow ratio for the NH_3 and ND_3 nitrides.

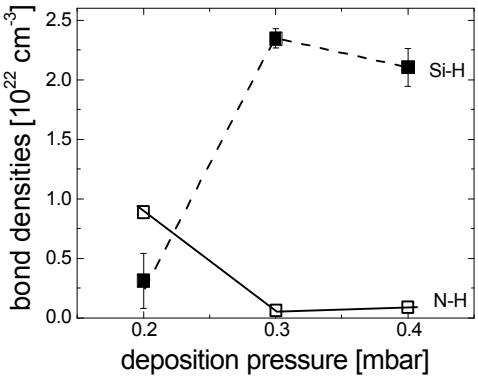

Figure 4: Si-H and N-H bond density versus the deposition pressure for N_2 nitrides.

The bond densities of the nitrides deposited with NH_3 (and ND_3) are stronger dependent on the flow ratio than those of nitrides deposited with N_2, especially at lower pressures (p = 0.2 mbar); the structural properties of N_2 layers depend mainly on the pressure. The increase in Si-N bond density (that we see for all nitrides) with increasing N/Si flow ratio is easily understood. At higher N/Si flow ratios relatively more reactive N-containing species are available; this will favor the formation of Si-N and N-H bonds over that of Si-Si and Si-H. The decrease in Si-H bonds with increasing N/Si flow ratio is only seen for the NH_3 and ND_3 nitrides. Mäckel and Lüdemann [13] found that the Si-N bond density increases (and the Si-H bond density decreases) with increasing N/Si atomic ratio in the layer. This corresponds to our results, since an increasing N/Si flow ratio will increase the N/Si atomic ratio in the layer.

The decrease of Si-N bond density for increasing pressures, also seen in all nitrides, is due to properties of our remote MW PECVD. In our system, the nitrogen containing gas is fed in near the plasma source, while the silane gas is fed in just above the samples. At the microwave source nitrogen (or ammonia) gas is dissociated by electron impact; while the silane in turn is dissociated by either electron impact or by interactions with N- or H- (in case of ammonia) radicals. Besides this, the dissociation of silane can be enhanced or even caused by the high temperatures in the deposition chamber. Higher pressures will confine the nitrogen plasma closer to the plasma source, and less reactive N-containing species will reach the substrate. This will cause the formation of more Si-rich SiN_x:H layers that are less dense. A more detailed description of the plasma chemistry can be found in other

publications [23,24].

The different flow and pressure dependence for both types of nitrides is caused by the difference in dissociation energy for N-N (9.81 eV) and H-NH_2 (4.65 eV) [25]. At low pressures, the degree of N_2 depletion will saturate for a certain microwave power; rendering the plasma independent on further increasing the N_2/SiH_4 flow ratio. Due to the lower ionization energy this maximum is not reached for NH_3. Within our processing parameters and the depletion of the NH_3 is close to 100% [17].

The lower Si-N bond density of the deuterated nitride, when compared to the nitride deposited with NH_3, is due to the difference in dissociation rate of NH_3 and ND_3. This dissociation rate depends on the vibration frequency of the N-D or N-H in the molecule, which is lower for N-D due to the larger mass. The Si-H bond density in the layers deposited with ND_3 is 75% of that in the corresponding layer deposited with NH_3, while the N-H bond density in layers made with ND_3 is hardly 50%. Since (in NH_3 and ND_3 nitrides) the majority of hydrogen is bonded to Si-atoms (see figure 3), this means that at least 25% of the hydrogen in the SiN_x:H layers stems from ammonia, while roughly 75% stems from silane.

In figure 5 the initial hydrogen fraction of all layers (deposited with N_2, NH_3 or ND_3) is shown against the Si-N bond density. We define the hydrogen fraction as:

$$\text{fraction H} = \frac{[\text{Si - H}] + [\text{N - H}]}{[\text{Si– H}] + [\text{N - H}] + [\text{Si – N}]} \qquad (1)$$

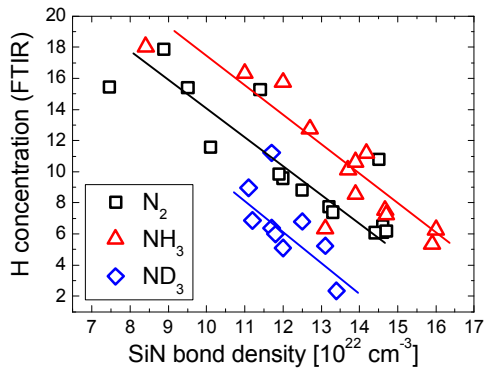

Figure 5: Total hydrogen concentration (calculated from bond densities) for the three different nitrides as a function of the Si-N bond density.

Although there is a lot of variation, the general trend is clear for all layers: with increasing Si-N bond density (and thus layer density) the total H-content decreases. For most SiN_x:H layers deposited with NH_3, more hydrogen is incorporated at the same Si-N bond densities than in layers deposited with N_2 or ND_3. As was found above, in layers deposited with ND_3 at least 25% of the hydrogen is replaced by deuterium. But, layers deposited with ND_3 also become less dense (lower Si-N bond density) using the same process parameters when compared with layers deposited with NH_3 due to the difference in dissociation rate, as was shown in figure 1. Both effects cause the H-content in ND_3 layers to be only 50% of the content in NH_3 layers at the same Si-N bond densities.

When N_2 is used instead of NH_3, the total H content decreases by roughly 25%. In this deposition, all hydrogen will stem from the silane; the 25% lower H-content is in agreement with the 25% difference in H-content between layers deposited with NH_3 and ND_3. This could mean that although the plasma chemistry is different, efficiency of hydrogen incorporation is approximately the same.

3.2 Bulk and surface passivation as a function of Si-N bond density

In previous publications we show that the Si-N bond density is a key parameter for bulk passivation [14,15,26]. Figure 6 shows the V_{oc} of cells made with SiN_x:H layers deposited with N_2 or NH_3. Wafers of average quality (A) and wafers of higher quality (B) were used. All values of V_{oc} are scaled to the maximum V_{oc} for each experimental run to be able to compare all the data.

From the figure it can be seen that:

- The V_{oc} for cells with SiN_x:H layers deposited with N_2 or NH_3 have the same dependence of the Si-N bond density.
- The maximum V_{oc} for both material qualities is found at the same Si-N bond density, viz. $1.3*10^{23}$ cm^{-3}. The difference is that for the better quality higher V_{oc} values are found for a broader range of Si-N bond densities.

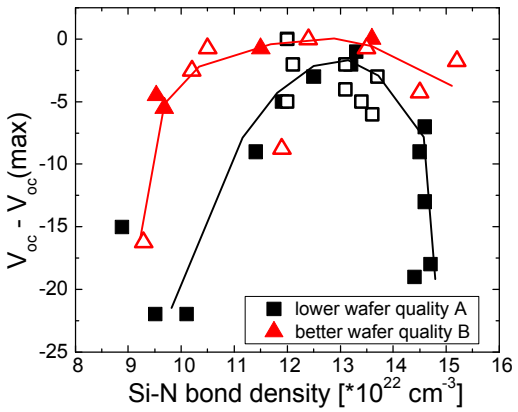

Figure 6: V_{oc}-V_{oc}(max) of mc-Si solar cells versus the Si-N bond density. The squares show the V_{oc} for cells made of average quality (A), the triangles show Voc for cells made of good wafer quality (B). Closed symbols: N_2 nitrides; open symbols: NH_3 nitrides. The lines are guides to the eye.

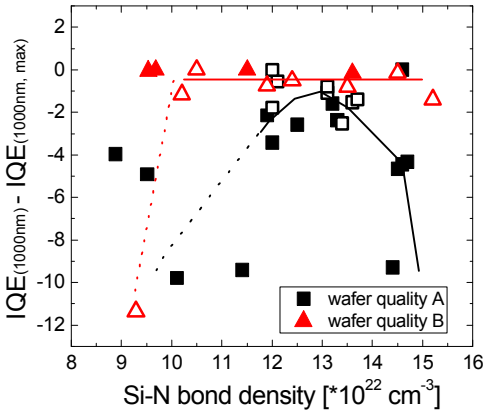

Figure 7: IQE at 1000 nm for the different solar cells. Again the difference between the different wafer qualities is clearly visible. Closed symbols: N_2 nitrides; open symbols: NH_3 nitrides. The lines are guides to the eye.

We were not able to make solar cells with [Si-N] < 9*10^{22} cm^{-3} or [Si-N] > 1.5*10^{23} cm^{-3}, because these layers became too inhomogeneous at larger areas.

V_{oc} is determined by both the bulk and surface passivation. To investigate the dependence of the Si-N bond density on bulk passivation the IQE at 1000 nm is shown in figure 7. When the wafer quality is lower (squares in graph 6 and 7), the V_{oc} follows the IQE at 1000 nm indicating V_{oc} is mainly influenced by the bulk properties of the solar cell. In the case of better wafer quality (triangles) however, the IQE remains constant down to very low Si-N bond densities (1*10^{23} cm^{-3}). In this case, the bulk properties remain constant and smaller changes in V_{oc} (<5 mV) are caused by differences in surface passivation; the better surface passivation for Si-N bond densities around 1*10^{23} cm^{-3} will be confirmed below. At the lowest bond densities, the drop in IQE reflects a drastic reduction in bulk passivation; this results in an additional loss in V_{oc} of about 10 mV.

The amount of surface passivation can be determined by measuring the effective lifetime of charge carriers in FZ wafers coated with SiN_x:H layers. In figure 8 we show the effective lifetimes for N_2 (closed symbols), and some NH_3 (open symbols) grown nitrides with the different Si-N bond densities, before and after a very long anneal (60 min at 800 °C) for the N_2 nitrides, and a shorter anneal for the NH_3 nitrides.

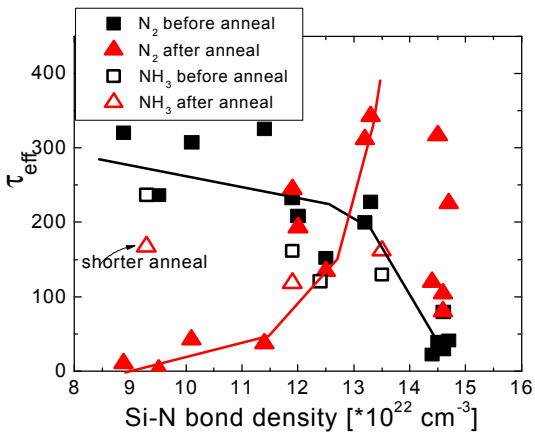

Figure 8: Effective lifetimes of charge carriers in FZ wafers with SiN_x:H layers before and after anneal (60 mins, 800 °C). N_2 nitrides: closed symbols, NH_3 nitrides: open symbols.

The figure shows that good initial surface passivation (large τ_{eff}) can be obtained for layers with low Si-N bond densities, but that this surface passivation is not thermally stable after a 60 minute anneal (although the much shorter firing of solar cells does not influence the τ_{eff} this much, see also arrow in figure 8 [23,27]). At high Si-N bond densities, the initial τ_{eff} is low, but after a long anneal the values improve drastically. Around [Si-N] ~ 1.3*10^{23} cm^{-3}, τ_{eff} remains constant at high values. At these bond densities, V_{oc} for wafers of good quality reaches its maximum (see figure 6, wafer quality B) that we contribute to the good and stable surface passivation. At higher Si-N bond densities there is a large variation in lifetime after annealing. This means that the best and most stable processing is found at a Si-N bond density of 1.3*10^{23} cm^{-3}, the same density as for best bulk passivation.

Combining the results for the bulk and surface passivation, we find optimum values for Si-N bond densities of $1.3*10^{23}$ cm^{-3} for both, regardless of the type of SiN_x:H used and regardless of the wafer quality.

3.3 Hydrogen diffusion in SiN_x:H layers.

In earlier publications we reported that the best surface and bulk passivation is found for denser layers, with a higher Si-N bond density ($1.3*10^{23}$ cm^{-3}), regardless of the initial amount of hydrogen. In these studies it was postulated that low Si-N bond densities result in more open structures that facilitate the formation of H_2 molecules that effuse into the ambient during anneal. This effused hydrogen will not contribute to the bulk passivation. In too dense layers ([Si-N] > $1.3*10^{23}$ cm^{-3}) the H-diffusion into the bulk of the solar cells during short anneals will be too small for good passivation [14,15,26]. In a recent publication, Dekkers et al [11] found that the mass density of the SiN_x:H layer governs the diffusion of hydrogen in the layer, denser layers prevent out-diffusion of molecular hydrogen. This publication confirms our earlier findings.

Our previous study on the H-diffusion in SiN_x:H and the related passivating properties was performed on SiN_x:H layers deposited with N_2 and SiH_4. This experiment is now extended with layers deposited with NH_3 and SiH_4. The diffusion of H in the NH_3 nitrides is monitored by measuring the Si-H and N-H bond densities as function of the anneal time at 800 ºC.

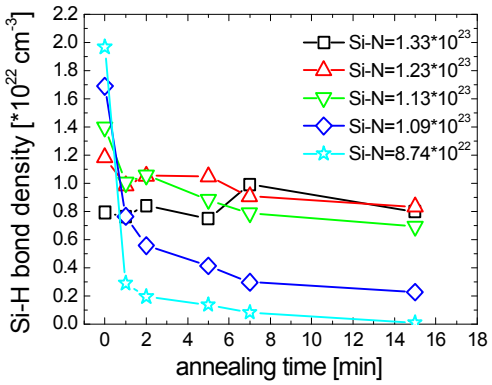

Figure 9: Change in Si-H bond density during anneal for different Si-N bond densities. All layers are deposited with NH_3 and SiH_4.

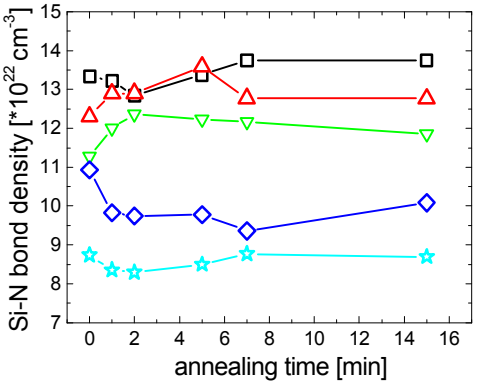

Figure 10: Change in Si-N bond density during anneal. All layers are deposited with NH_3 and SiH_4. The symbols correspond to those in figure 9.

In figure 9 the change in Si-H bond density upon annealing at 800 ºC is shown for layers with different Si-N bond densities, deposited with SiH_4 and NH_3. The N-H bond density shows similar behavior as a function of time. It is clear that layers with a high initial H-concentration (low Si-N bond density) loose most hydrogen during anneal. In figure 10 the change in Si-N bond density during the same anneal times is shown. Although some changes may be seen during the first anneal periods, the Si-N bond density remains approximately constant during anneal.

Similar to the N_2 nitrides [14,15], also in NH_3 nitrides the H-diffusion shows a strong time-dispersive (time dependent diffusion coefficient) behavior. This effect is well known for H diffusion in a-Si:H and can be described by [28]:

$$C_H = C_{H,0}\exp(-\pi^2 D_H t/L^2) \qquad (2)$$

$$D_H(t) = D_H(0)\{\omega t\}^{-\alpha} \qquad (3)$$

ω is the H attempt-to-diffuse frequency and α is the temperature dependent dispersion parameter ($0 < \alpha < 1$). More details about this dispersive character of H diffusion in SiN_x:H can be found in [24].

The initial diffusion coefficient D_1 of the hydrogen strongly depends on the Si-N bond density in the layers. In figure 11, these coefficients for Si-H for both N_2 and NH_3 nitrides are shown. The coefficients for N-H bond densities are similar, but harder to measure since the peak is much smaller and the error much larger. Although the hydrogen concentrations are quite different for N_2 and NH_3 nitrides (see figure 5), the diffusion coefficients are the same for both materials, and only depend on the Si-N bond densities.

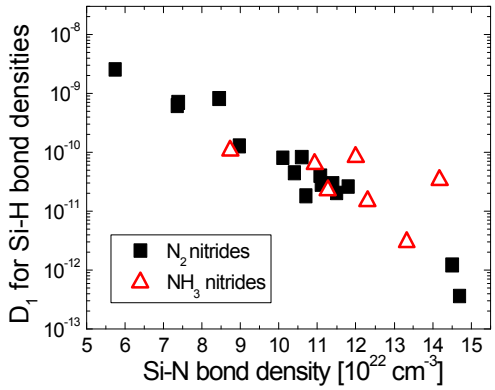

Figure 11: Initial Si-H diffusion coefficient D_1 as a function of Si-N bond density.

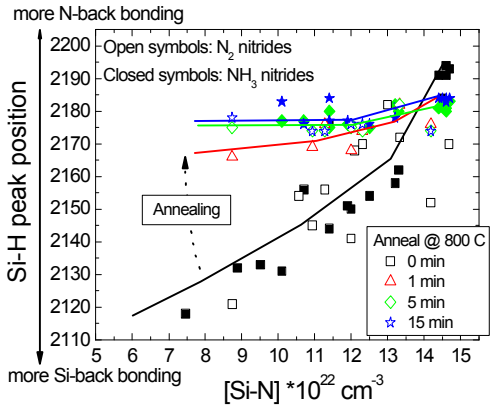

Figure 12: Shift in Si-H peak position as a function of annealing time.

A similar agreement between N_2 and NH_3 nitrides is also found for the shift in the Si-H peak position, shown in figure 12. The Si-H peak position is shown for both N_2 and NH_3 nitrides before and after annealing at several times. The Si-H peak position depends only on the Si-N bond density and the anneal times. The Si-H stretch vibration mode in SiN_x:H can occur at various frequencies between 2000 and 2300 cm^{-1}, depending on the back bonding of the concerning Si atom. If the back bonds are mainly Si atoms the vibration frequency is low (2000 cm^{-1} for H-Si-Si_3), in the case of mainly N atoms the vibration frequency is high (2220 cm^{-1} for H-Si-N_3) [21,22]. As expected, before annealing (t = 0; square symbols) we see that if the Si-N bond density is low, thus more Si in the layer, the Si-H back bonding is mainly silicon. When the Si-N bond density is high (more N in the layer), the Si-H back bonding is mainly nitrogen.

In figure 12 we see that after annealing the Si-H bonds with Si-rich back bonding disappear from all nitrides, only the Si-H bonds with N-rich back bonding remain. Indeed, figure 11 shows that SiN_x:H layers with low Si-N bond densities and thus more Si-rich back bonding have the highest Si-H diffusion coefficient. This stems from the more open and porous structure of the Si-rich layers. The strongest and most stable bonds are those around 2180 (H-Si-HN_2).

Although the N_2 and NH_3 nitrides are formed with different deposition mechanics and the initial hydrogen concentrations are not the same, the hydrogen diffusion and corresponding structural changes are the same for layers with the same Si-N bond density. In paragraph 3.2 we already showed that the bulk passivating properties of the two layers depend in the same way on the Si-N bond density; this fact can now be explained by the similar H diffusion from the SiN_x:H layer into the mc-silicon due to the same Si-N bond density in the layers.

4. CONCLUSIONS

We have shown that for SiN_x:H layers deposited with our remote MW PECVD system the N/Si flow ratio and the deposition pressure are important processing parameters. The Si-N, Si-H and N-H bond densities of layers deposited with N_2, NH_3 or ND_3 are related to N/Si flow ratio and the pressure *p* in a similar way, but the difference in dissociation energy and rate causes differences in the deposition mechanisms. Comparing the Si-N and Si-H bond densities found for NH_3 and ND_3 grown layers, we find that roughly 25% of the hydrogen in the SiN_x:H layers stems from the ammonia precursor gas, while 75% stems from the silane. This fact is confirmed by the 25% difference in H-content in N_2 and NH_3 layers.

Even though the N_2 and NH_3 nitrides are formed with different deposition mechanics and the initial hydrogen concentrations are not the same, the hydrogen diffusion and thus bulk passivation are the same for layers with the same Si-N bond density. Layers with low Si-N bond densities are porous with large hydrogen diffusion coefficients. During anneal the hydrogen will effuse into the ambient in molecular form and will not contribute to the passivation. Dense layers on the other hand, with high Si-N bond densities have very low diffusion coefficients. For too high Si-N bond densities the diffusion of the atomic hydrogen in the SiN_x:H layer will be too slow, resulting in less passivation during short anneals. The similar H-diffusion from the SiN_x:H layer explains the fact that we find optimum values for bulk passivation for the same Si-N bond densities of $1.3*10^{23}$ cm^{-3} for both N_2 and NH_3 nitrides and regardless of the starting wafer quality. Also the best surface passivation is found for both nitrides around this Si-N bond densities of $1.3*10^{23}$ cm^{-3}.

Consequently, the Si-N bond density found via the FTIR analysis is an important parameter for the solar cell characteristics, related to both the bulk and surface passivation of the SiN_x:H layers, regardless of the type of SiN_x:H. This study therefore indicates that FTIR analysis of the SiN_x:H layers gives us a quick and reliable tool to check the quality and properties of different SiN_x:H layers. This will allow optimization of SiN_x:H deposition processes and systems without having to make complete solar cells.

5 ACKNOWLEDGEMENTS

This work was partly financially supported by NovemSenter in the DEN program, and the FP6 European Crystal Clear project (EC contract SES6-CT-2003-502583).

6 REFERENCES

[1] S. Winderbaum, F. Yun, O. Reinhold, J. Vac. Sci.Techn. A 15, 1020 (1997).
[2] Z. Chen, A. Rohatgi, R.O. Bell, J. P. Kalejs, Appl. Phys. Lett. 65, 2078 (1994)
[3] F. Duerinckx, J. Szlufcik, Sol. Energy. Mat. Sol. Cells, 72, 231 (2002)
[4] W.J. Soppe, C. Devilee, S.E.A. Schiermeier, J. Hong, W.M.M. Kessels, M.C.M. Van de Sanden, W.M. Arnoldbik, A.W. Weeber, *Proceedings of the 17th European Photovoltaic Solar Energy Conference, 22-26 October 2001, Munich, Germany*: 1543-1546
[5] A. Aberle, Crystalline silicon solar cells – Advanced Surface Passivation and analysis, UNSW, Sydney (1999); Progress in Photovoltaics: Research and Applications 8, 473 (2000)
[6] W.M. Bik, R.N.H. Linssen, F.H.P.M. Habraken, W.F. van der Weg, A.E.T. Kuiper, Appl. Phys. Lett. 56, 2530 (1990)
[7] M. Maeda and M. Itsumi, J. Appl. Phys. 84, 5243 (1998)
[8] G. C. Yu and S.K. Yen, Appl. Surf. Sci. 201, 204 (2002)
[9] C. Boehme and Lucovski, J. Non-Cryst. Sol. 299, 1157 (2002); J. Appl. Phys. 88, 6055 (2000)
[10] J. Hong, W.M.M. Kessels, W.J. Soppe, A.W. Weeber, W.M. Arnoldbik, M.C.M. Van de Sanden, J. Vac. Sci. Techn. B: 21, 2123 (2003)
[11] H. F. W. Dekkers, L. Carnel, G. Beaucarne, W. Beyer, *Proceedings of the 20th European Photovoltaic Solar Energy Conference, 6-10 june 2005, Barcelona, Spain*
[12] J. Tan, A. Cuevas, S. Winderbaum, K. Roth, *Proceedings of the 20th European Photovoltaic Solar Energy Conference, 6-10 june 2005, Barcelona, Spain*
[13] H. Mäckel and R. Lüdemann, J. Appl. Phys. 92, 2602 (2002)
[14] A.W. Weeber, H.C. Rieffe, W.C. Sinke, W.J. Soppe, *Proceedings of the 19th European Photovoltaic Solar Energy Conference, 7-11 june 2004, Paris, France:* p1005
[15] A.W. Weeber, H.C. Rieffe, I.G. Romijn, W.C. Sinke, W.J. Soppe, *Proceedings of the 31st IEEE Photovoltaic Specialists Conference, 3-7 jan 2005, Orlando, USA*
[16] R. A. Sinton, A. Cuevas, Appl. Phys. Lett 69, 2510 (1996)
[17] W. J. Soppe, B.G. Duijvelaar, S.E.A. Schiermeier, A.W. Weeber, A. Steiner, F.M. Schuurmans, *Proceedings of the 16th European Photovoltaic Solar Energy Conference, 1-5 may 2000, Glasgow, Scotland*
[18] N. Maley, Phys. Rev. B 46, 2078 (1992)
[19] F. Giorgis, F. Giuliani, C.F. Pirri, E. Tresso, C. Summonte, R. Rizzoli, R. Gallloni, A. Desalvo, P. Rava, Phil. Mag. B 46, 2078 (1992)
[20] E. Bustarret, M. Bensouda, M.C. Habrard, J. C. Bruyere, S. Poulin, S.C. Gujrathi, Phys. Rev. B 38, 8171.
[21] W. J. Soppe, J. Hong, W.M.M. Kessels, M.C.M. van der Sanden, W.M. Arnoldbik, H. Schlemm, C. Devilee, H. Rieffe, S.E.A. Schiermeier, J.H. Bultman, A.W. Weeber, *Proceedings of the 29th IEEE Photovoltaic Specialists Conference, 20-24 may 2002*, New Orleans, USA
[22] A.J.M. van Erven, Master Thesis, Eindhoven University of Technology
[23] W. Soppe, H.C. Rieffe, A.W. Weeber, Progress in Photovoltaics: Research and Applications, in press
[24] W. Soppe, H.C. Rieffe, I.G. Romijn, W.C. Sinke, A.W. Weeber, to be published
[25] D. L. Lide, CRC Handbook of Chemistry and Physics, CRC Press, Boca Raton (1994)
[26] I. G. Romijn, W.J. Soppe, H.C. Rieffe, A.R. Burgers, A.W. Weeber, *Proceedings of the 20th European Photovoltaic Solar Energy Conference, 6-10 june 2005, Barcelona, Spain*
[27] A. Weeber, H.C. Rieffe, M.J.A.A. Goris, J. Hong, W.M.M. Kessels, M.C.M. van de Sanden, W.J. Soppe, *Proceedings of the 3rd World Conference on Photovoltaic Energy Conversion, 11-18 may 2003, Osaka, Japan*
[28] W. Beyer, Sol. Energy Mat. Sol Cells 78, 235 (2003)